Hindawi
International Journal of Chemical Engineering
Volume 2024, Article ID 3463252, 12 pages
https://doi.org/10.1155/2024/3463252

Research Article

Flexible Polycarbonate and Copoly(Imide-Carbonate)s-Based Frequency Selective Surface for Electromagnetic Shielding Application

A. Murugesan,[1,2] **S. Ramprabhu**,[3] **and P. Senthil Kumar**[4]

[1]*Polymer Science and Engineering Lab, Department of Chemistry, Sri Sivasubramaniya Nadar College of Engineering, Kalavakkam 603110, Tamil Nadu, India*
[2]*Centre of Excellence in Water Research (CEWAR), Sri Sivasubramaniya Nadar College of Engineering, Kalavakkam 603110, Tamil Nadu, India*
[3]*Department of Electronics Engineering, Madras Institute of Technology Campus, Anna University, Chennai 600044, Tamil Nadu, India*
[4]*Centre for Pollution Control and Environmental Engineering, School of Engineering and Technology, Pondicherry University, Kalapet, Puducherry 605014, India*

Correspondence should be addressed to A. Murugesan; murugesana@ssn.edu.in and P. Senthil Kumar; senthilkumarp@ssn.edu.in

Received 11 October 2022; Revised 24 December 2023; Accepted 8 March 2024; Published 3 April 2024

Academic Editor: Selvaraju Narayanasamy

Optically transparent polycarbonates (PCs) and Copoly(Imide-Carbonate)s (Co-PICs) were synthesized by the melt polycondenzation method. Rigid (imide) and flexible (-O- and $-C(CH_3)_2-$) moieties were incorporated in the structure of bisimide diol comonomer using 4-aminophenol and 4,4′-(4,4′-isopropylidenediphenoxy) bis(phthalic anhydride). The structural properties of synthesized comonomers and polymers were confirmed by ^1H, ^{13}C-NMR and FT-IR spectra. Thermal properties of polycarbonates and copolycarbonates were examined using DSC and TG analysis. Thermal properties (glass transition (T_g) and thermal decomposition (T_d) temperature) of copolymers were enhanced without sacrificing properties of BPA-based PC (high transparency, ductility, and processability) by the incorporation of active functional bisimide diol comonomer (5–10 mole %) in the polycarbonate backbone. Different sets of PCs and Co-PICs thin film substrates were prepared by the solvent casting method and used to design frequency selective surface. The proposed flexible FSS offers shielding of 20 dB at 8.8 GHz. In addition, the FSS offers polarization independent operation with its symmetrical unit cell geometry.

1. Introduction

During the recent decades, different aspects of the synthesis of new copolymers are very important and potential class of materials which find wide applications as high-performance engineering polymers [1–3]. Aromatic polycarbonates (PCs) constitute continue to receive much attention in the FSS substrate for electromagnetic shielding application because of their good optical transparency, high glass transition temperature, good solubility in halogenated solvents ($CHCl_3$), processability, and thermal and mechanical properties [4–13]. In recent years, there has been extensive research to improve the heat resistance of PCs. This can be achieved by either restricting the conformational mobility of the carbonate moiety or increase in persistent length of the polymer. Use of tetra methyl bis-phenol A as a monomer is an example of the former approach, whereas copolymer with ester monomer is an example of the latter approach [14]. Bisphenol- A (BPA)-based PCs (BPA-DPC (diphenyl carbonate)) are having Tg around 145°C, which can be modified in the incorporation of the different functional and bulky groups in the derivate of the BPA. Design of mechanically robust high T_g(180–230°C) polymers has been accomplished by copolymerization with 1, 4-cyclohexanedicarboxylic acid [15]. The most successful approach to high heat PCs is by incorporating 4, 4`- (3, 3, 5 -trimethylcyclohexylidene

diphenol) (T_g (240–283°C)) as the comonomer [16, 17]. The *gem*-dimethyl (T_g (198–275°C)) group at the 3-position is believed to be responsible for the observed property improvement. High heat properties are achieved without sacrificing properties of PC, such as high transparency, high ductility, and processability [18–28]. In corporation of rigid (imide), flexible (cyclic ring), and side chain (bulky groups) via commoner might be an effective way to achieve higher thermal and mechanical properties, and this could be focused in the article. Introduction of heterocyclic imide (BPA derivative) moiety with flexible (ether, methyl, phenyl, etc.) and rigid (imide) groups into the structure of the high-performance polymers to improve the thermal properties as well as processability of the copolymers. To overcome the issue, a new molecule is required to enhance the thermal and mechanical properties of polymers. [29–31].

Electromagnetic pollution is of serious concern nowadays due to intensive networking. The impact of which tends to increase with the concept of Internet of Things (IoT) gathering momentum. Frequency selective surfaces (FSSs) are extensively used for shielding applications. Flexible substrate-based FSSs have gained much attention owing to its conformal geometry. However, so far, glassy epoxy resins (GER) have been used extensively as the substrate material to design the FSS, but these materials are highly rigid, opaque, and brittle in nature. A new versatile material is needed to solve this problem. Flexible polymer substrate has been seemed as the alternative and promising material to replace the currently used rigid GER [32–35].

In this research work, the easy synthetic accessibility to a class of imide containing bisphenol A in the course of our study on thermal rearrangement led us to explore the utility of this class of monomers for polycarbonate. Such monomers have not been reported as comonomers for polycarbonates. Incorporation of flexible (-O- and $-C(CH_3)_2-$) and rigid (imide) and moieties in the PCs' backbone has improved the thermal (T_g and thermal degradation) properties. The excellent Co-PICs are used as a substrate to design a flexible FSS for conformal electromagnetic shielding applications.

2. Experimental

2.1. Materials. 4-aminophenol, bisphenol A, and diphenylcarbonate (Sigma Aldrich, India) were purified by sublimation prior to use. 4,4′-(4,4′-isopropylidenediphenoxy) bis (phthalic anhydride) (Sigma Aldrich, India) was purified by sublimation. Sodium sulfate (Na_2SO_4) and sodium hydroxide (NaOH) and tetramethylammonium hydroxide (TMAH) (extrapure AR) were procured from SRL, India. Ethanol, methanol, N-methyl pyrrolidine (NMP), pyridine, toluene, and chloroform (AR grade) were received from Thomas Baker, India, and purified prior to use as per literature procedure.

2.2. Measurements. Melting points were determined by the open capillary tube method. FT-IR analysis was carried out using KBr pellet and the spectral range of 4000–450 cm^{-1} on a Bruker Tensor 27 spectrometer. NMR spectra were recorded on a Bruker 400 MHz spectrometer at a resonance frequency of 400 MHz for ^1H and ^{13}C using $CDCl_3$ and DMSO-d_6 as a solvent. Thermogravimetric analysis was performed on a Perkin-Elmer TGA-7 system at a heating rate of 10°C/minute under nitrogen atmosphere. Differential scanning calorimetry (DSC) analysis was carried out on TA Instruments DSC Q10 at a heating rate of 10°C/minute in nitrogen atmosphere. The intrinsic viscosities were measured with an Ubbelohde viscometer at 25 ± 0.1°C in chloroform. GPC (gel permeation chromatography) type of liquid chromatography was used to determine the number (M_n) and weight (M_w) average molecular weight of the polymers and as well as poly dispersive index (PDI). The analysis was performed with Copoly(Imide-Carbonate)s [Co-PICs-1 and Co-PICs-2] samples in THF solvent, and the solution is injected into a chromatography column to measure the parameters. The optical transparency of PC (1), Co-PICs-1 (2), and Co-PICs-2 (3) was measured using UV-spectroscopy with wavelength from 200 to 800 nm.

2.3. Synthesis of Bisimide Diol Comonomers. Synthesis of comonomer reaction is represented in Scheme-I**.** 4-aminophenol (2.099 g, 19.204 mmol) was dissolved in N-methyl pyrrolidone (NMP) (50 mL) and toluene (50 mL) in a 500 mL round bottom flask fitted with a Dean–Stark trap, reflux condenser, and nitrogen purge. 4,4′-(4,4′-isopropylidenediphenoxy) bis (phthalic anhydride) (5.0 g, 9.6063 mmol) was added under stirring at 0–5°C for 1 h. A small exotherm was observed during formation of the amic acid. The reaction was allowed to proceed at 30°C for 1 h and then refluxed (160°C) for 12 h to remove the water of imidization as a toluene-water azeotrope[1]. Excess toluene was then removed by distillation. After cooling, the flask contents were slowly poured into methanol/water (200 mL, 1 : 1 mixture by volume). The white precipitate was collected by filtration and washed with water. The product was recrystallized from ethyl acetate and dried at 100°C for 48 h in a vacuum. The bisimide diol was used as a comonomer for the synthesis of copolycarbonates and which is not yet reported. Yield 6.7 g, 99%; mp 262–263°C (white).

^1H-NMR (DMSO-d_6) $\delta = 9.79$ (2H, -OH), 8.34 ($CDCl_3$ impurity with DMSO-d_6) 7.93–7.97 (2H, ArCH), 7.34–7.43 (8H, ArCH), 7.13–7.23 (8H, ArCH), 6.87–6.91 (4H, ArCH), 3.35 (Solvent ($CHCl_3$)), 2.53 (H_2O), and 1.74 (6H, CH_3) ppm).

^{13}C-NMR (DMSO-d_6) $\delta = 166.9, 162.9, 157.4, 152.7, 147.2, 134.4, 128.8, 125.5, 123.0, 119.9, 115.6, 111.6, 42.2$, and 30.7 ppm.

Elemental analysis: calculated for $C_{31}H_{16}F_6N_2O_6$, C (73.50%), H (4.30%), N (3.99%); found, C (72.90%), H (4.28%), N (4.07%).

2.4. Synthesis of Polycarbonates and Co-Poly(Imide-Carbonate)s (Co-PICs). The polycarbonates were synthesized according to the following general procedure, and the polymerization reaction is shown in Scheme-II. A glass reaction tube equipped with a Claisen distiller and a nitrogen gas inlet and outlet were filled with a homogeneous solid mixture composed of (1 g, 4.380) mmol bisphenol A,

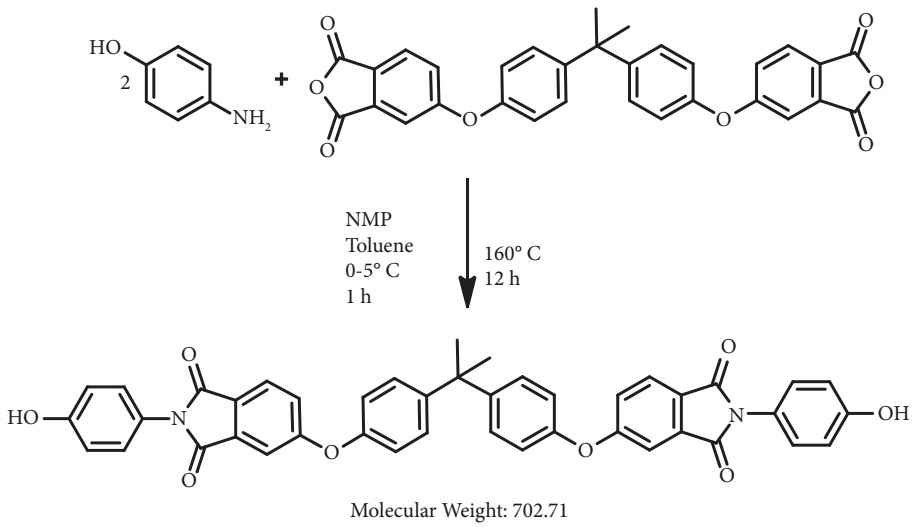

Scheme 1: Synthesis of comonomer.

(1.0134 g, 4.7308 mmol) diphenylcarbonate, NaOH (2.19 μl), and tetramethylammonium carbonate (2.628 μl). The reaction mixture was heated in a salt bath at 180°C under a stream of nitrogen gas for 2 h. The temperature of the bath was increased to 200°C with pressure at 180 mmHg for 25 min, the pressure was reduced to 100 mmHg, and the reaction was kept for 45 min. The reaction was then heated at 220°C for 5 min after that the pressure reduced to 15 mmHg and then reaction continue for 45 min. The reaction was then heated at 250°C for 5 min after that the pressure reduced to 2 mmHg and then the reaction continued for 45 min. The temperature was gradually increased to 300°C, and the pressure was reduced to 0.1 mmHg, and then the reaction continued for 2 h to remove the byproduct phenol in the polycondenzation reaction. After 1 h, the glass reaction tube was cooled, and the formed polymer was dissolved in chloroform. The solution was filtered, and the polymer was precipitated by dropwise addition to methanol as a non-solvent. The resulting polymer was filtered and dried in a vacuum at 80°C for 24 h.

Yield: 1.02 g (97.27%) (white); the copolycarbonates (Co-PICs-**1**) were synthesized according to the abovementioned general (synthesis of polycarbonates) procedure[2-5], and the polymerization reaction is shown in Scheme 3. 1.8999 g, (8.3225 mmol (95%)) bisphenol A (BPA), 0.3078 g, (0.4380 mmol (5 mole %)) of the abovesynthesized bisimide diol comonomer, 2.0268 g (9.4614 mmol) diphenylcarbonate (DPC), sodium hydroxide (NaOH) solution (4.38 μl, 0.001 M), and tetramethylammonium hydroxide (TMAH) solution (5.250 μl (0.221 M)). Yield 2.30 g, 99% (white coloured fiber); ^{1}H NMR ($CDCl_3$) δ = 7.06–7.93 (8.74 H, ArCH) and 1.71 (6H, CH_3) ppm.

Similarly, Co-PICs-**2** [1.8000 g (8.3223 mmol (90%)) of bisphenol A, 0.6156 g, (0.8760 mmol (10 mole %)) of the abovesynthesized bisimide diol comonomer, 2.0268 g (9.4617 mmol) of DPC, (NaOH) (4.38 μl, 0.001 M), and (TMAH) (5.250 μl (0.221 M))] was synthesized, yield 2.19 g, 99% (white);

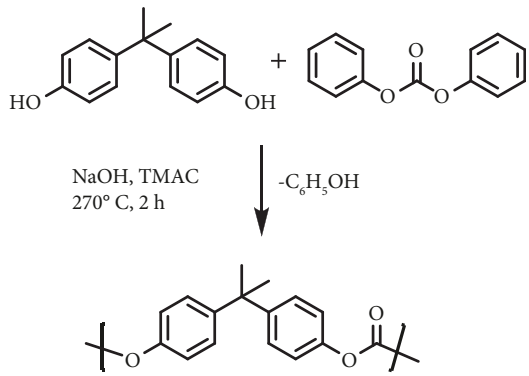

Scheme 2: Synthesis of polycarbonates.

^{1}H NMR ($CDCl_3$) δ = 7.06–7.93 (9.44 H, ArCH) and 1.71 (6H, CH_3) ppm.

Similarly, Co-PICs-**3** [1.7000 g (8.3223 mmol (85%)) of bisphenol A, 0.9234 g, (0.8760 mmol (15%)) of comonomer, 2.0268 g (9.4617 mmol) of DPC, (NaOH) (4.38 μl, 0.001 M), and (TMAH) (5.250 μl (0.221 M))] were synthesized, Yield 2.01 g, 91% (pale yellow); but it thin film also pale yellow in nature and loss the PC properties. There is a limitation in the incorporation of comonomers in the structure of co-polymers, after 20 mole percentage of comonomer incorporation loss of the properties of PCs. Due to such reasons, Co-PIC-3 was not used for further process.

3. Results and Discussion

3.1. Synthesis and Characterization of Bisimide Diol Comonomer. 4-aminophenol was reacted with 4,4′-(4,4′-Isopropylidenediphenoxy) bis (phthalic anhydride) in the presence of NMP solution at 0–5°C to form amic acid as an intermediate. This intermediate undergoes thermal imidization at 160°C to give bisimide diol comonomer with elimination of byproduct (water) using water-toluene azeotrope mixture. The structure of comonomer was characterized by NMR and

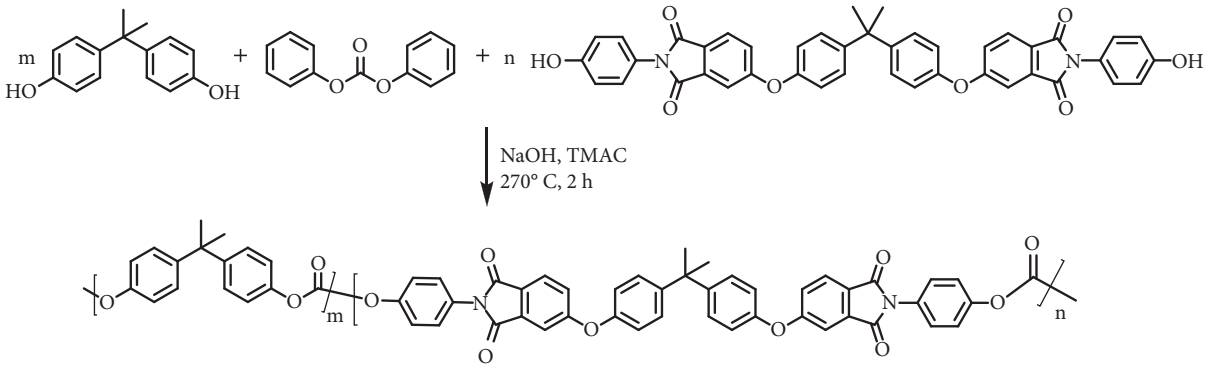

Scheme 3: Synthesis of Copoly(Imide-Carbonate)s (Co-PICs).

elemental analysis. From the ^{1}H-NMR spectrum of monomer (Figure 1), the –OH and aromatic proton peaks were observed at δ value 9.79 and 6.78–7.97 ppm, respectively. 4-aminophenol "c" and "d" protons are overlapped with "c" and "d" protons of anhydride due to proton shielding effects, which is mentioned in Figure 1. $CDCl_3$ was used as a cosolvent, whose peaks are observed at δ value 9.79 ppm. DMSO-d_6 solvent and moisture (water) proton peaks were obtained at δ value 2.53 and 3.5 ppm, respectively. From the ^{13}C-NMR spectrum (Figure 2) of monomer, carbonyl (C=O), ether linkage (-C-O-C-), and hydroxyl group (-C-OH) carbon peaks were observed at δ value 166.9, 162.9–157.4, and 152.7 ppm, respectively. Aromatic and aliphatic carbon peaks were obtained at δ value 147.2-111.6 and 42.2–30.7 ppm, respectively. The NMR spectra result of comonomer could be confirmed by the chemical structure of bisimide diol (5,5′-(4,4′-propane-2,2′-diyl) bis(4,1-phenylene) bis(oxy)bis(2–(4-hydroxyphenyl) isoindoline-1,3-dione)) and was further confirmed by elemental analysis.

3.2. Synthesis and Characterization of Polycarbonates. The FT-IR spectra of bisphenol A (BPA), diphenyl carbonate (DPC), and polycarbonate (PC) are shown in Figure 3. The analysis was carried out using the KBr pellet and the spectral range of 4000-450 cm^{-1}. The assignments of the peaks of bisphenol A are (cm^{-1}): (3350) -OH stretch (3068 and 3027) ArCH stretch, (2960) CH stretch (methyl), (1889) p-sub, (1600, 1500, and 1447) C=C stretch phenyl group, (1360), (1232 and 1170) -$(CH_3)_2$-. Similarly, the assignments of the peaks of diphenyl carbonate are (cm^{-1}): (3058) ArCH stretch, (1776, 1258 and 1176) -O-CO-O-, (1592 and 1494) phenyl, (1258) C-O stretch.

From the FT-IR spectrum of polycarbonate, disappearance of phenolic peaks (3350 and 1304 cm^{-1}) and appearance of all other peaks (carbonate, ArCH, (-$(CH_3)_2$–) could confirm that the respective functional groups are present in the structure of polycarbonate in the polymer backbone. The structure of the polycarbonate could be further confirmed by the NMR spectrum.

The ^{1}H-NMR spectrum of bisphenol A is shown in Figure S1. The assignments of the peaks of bisphenol A are ^{1}H-NMR (DMSO-d_6 and $CDCl_3$) $\delta = 8.22$ ppm (2H, -OH), $\delta = 6.90$–6.95 ppm (4H, ArCH), $\delta = 6.59$–6.64 ppm (4H, ArCH), and $\delta = 1.48$ ppm (6H, -CH). The signals at $\delta = 2.52$ and 7.25 ppm are due to DMSO-d_6 and $CDCl_3$, respectively. ^{1}H-NMR analysis of bisphenol A confirms that exact protons are appearing in the structure of bisphenol A. Similarly, diphenyl carbonate structure is also analyzed by ^{1}H-NMR analysis. Figure S2 shows the ^{1}H-NMR spectrum of diphenylcarbonate. From this spectrum, aromatic proton peaks only observed in the range of $\delta = 6.96$–7.25 ppm (10H, ArCH). The ^{1}H-NMR analysis of DPC confirms the structure of diphenyl carbonate.

From the ^{1}H-NMR spectrum of polycarbonate (Figure S3), disappearance of phenolic –OH protons [$\delta = 8.22$ ppm (2H, -OH)] and appearance of tertiary methyl [$\delta = 1.68$ ppm (6H, -CH)] and ArCH [$\delta = 7.13$–7.27) ppm (6H, ArCH)] protons could suggest that the corresponding protons of polycarbonate are presented in the structure of the polymer. This structure could be further confirmed by ^{13}C-NMR (Figure S4) analysis.

3.3. Synthesis and Characterization of Co-PICs. Copoly(Imide-Carbonate)s [Co-PICs-1 and Co-PICs-2] were synthesized with DPC, BAP, and bisimide diol comonomer (5 and 10 mole %) by melt polycondenzation method sodium hydroxide and tetramethylammonium hydroxide as a catalyst [36–38]. The ^{1}H-NMR spectra of the Co-PICs- 1 and 2 are shown in Figures 4 and 5, respectively. From the ^{1}H-NMR spectra of PC and Co-PICs, the ratio of aromatic and aliphatic protons was integrated. The obtained integration values of aromatic and aliphatic protons of polycarbonates and Copoly(Imide-Carbonate)s are nearly close to the calculated values (values are calculated according to the mole ration of commoners). The ^{1}H-NMR peak intensity results show that the appropriate percentage of the imide functional moiety was incorporated in the polymer backbone. The intrinsic viscosity [η] of Co-PICs was determined at a different concentration such as 0.1, 0.2, 0.3, 0.4, and 0.5 g·dl^{-1} in $CHCl_3$ as a solvent at 25°C for Co-PICs-1 (0.66) and Co-PICs-2 (0.64). The molecular weights of Co-PICs-1 and Co-PICs-2 are found to be 380189 and 363078 g/mol, respectively, using the Mark Houwink empirical equation. The PDI values of Co-PICs-1 and Co-PICs-2 are found to be using number average molecular weight (M_n, derived from GPC result) 6.33 and 5.10, respectively (Table 1).

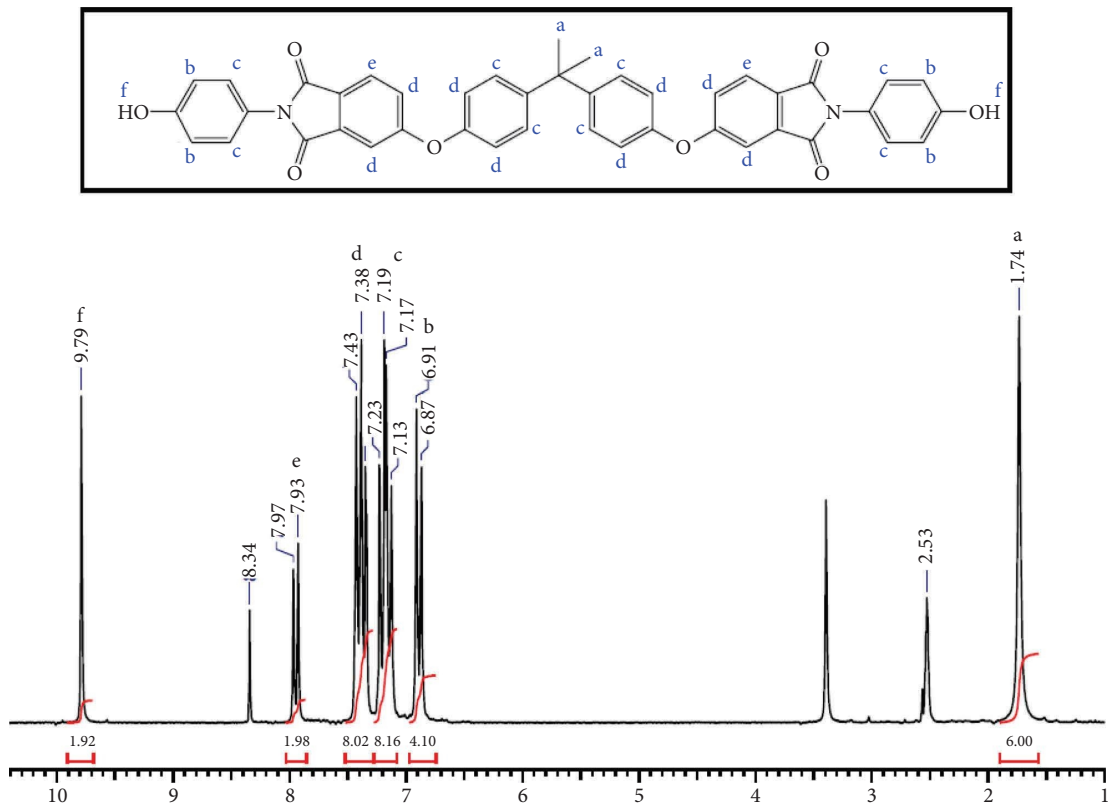

Figure 1: ^{1}H-NMR spectrum of comonomer.

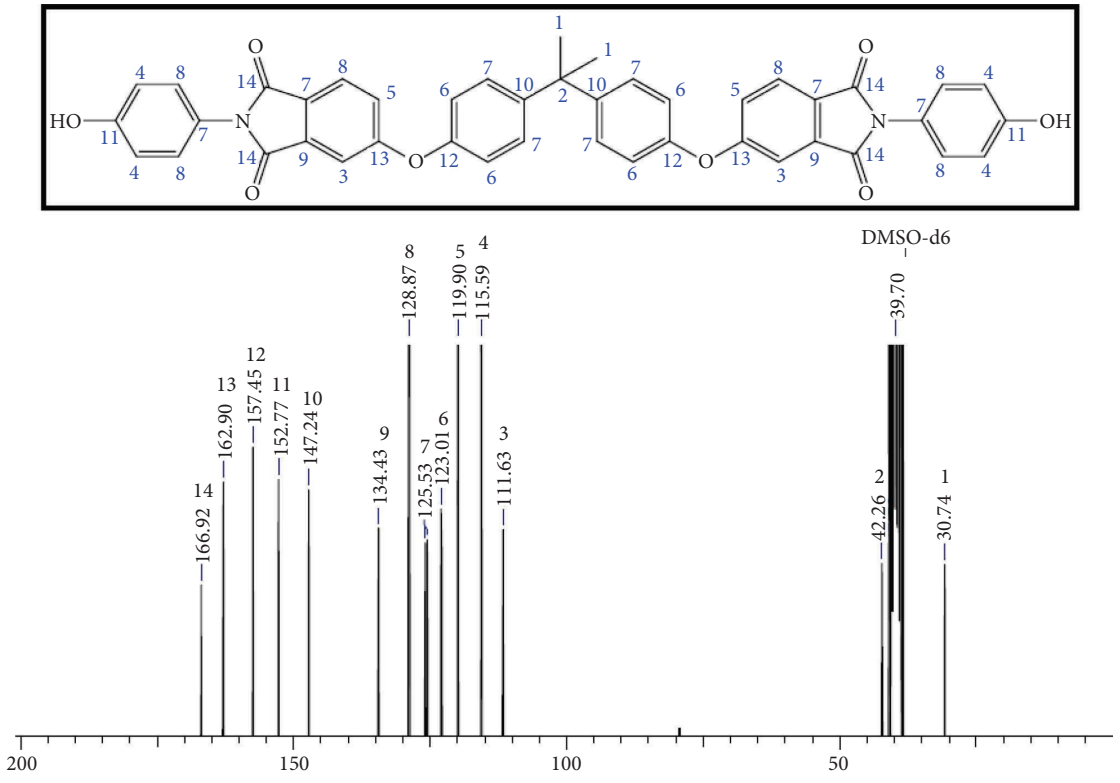

Figure 2: ^{13}C-NMR spectrum of comonomer.

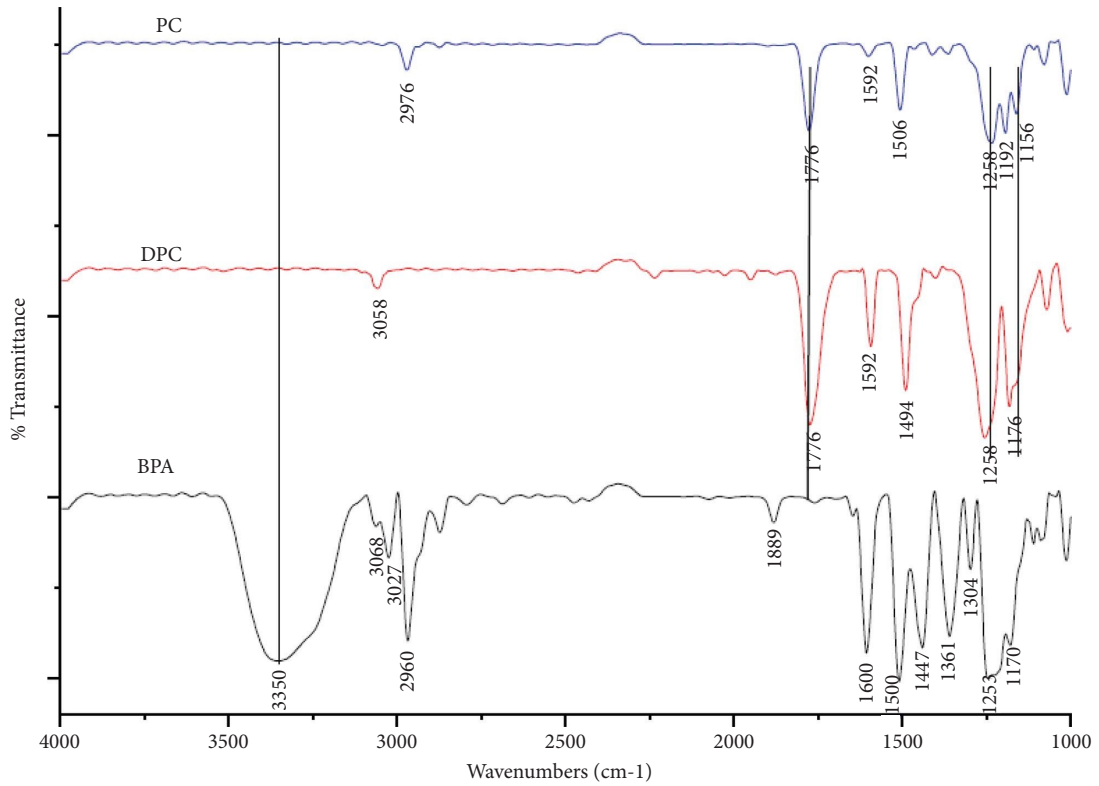

Figure 3: FT-IR spectra of bisphenol A (BPA), diphenylcarbonate (DPC), and polycarbonate (PC).

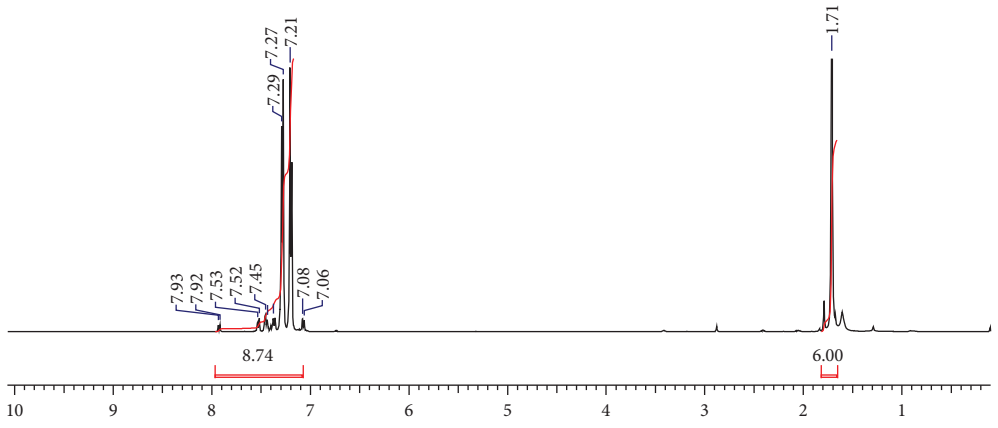

Figure 4: ^{1}H-NMR spectrum of Co-PICs-1.

The spectrum of gas permeable chromatograms was analyzed using the THF solvent and is shown in Figure 6. Two different narrow distributions of sharp peaks were observed in the spectra, which confirm that different molecular weight polymers such as imide and carbonate moieties are present in the structure of the copolymers. This result is also a strong evidence to confirm the incorporation of imide and carbonate functional moieties in the structure of the copolymers and as well as random polymerization. From the GPC analysis, M_n, M_w, and PDI were determined and data are listed in Table 1. The M_n values of Co-PICs-1 and Co-PICs-2 are found to be 6000 and 7110 g/mol, respectively. Similarly, M_w was measured to be 376009 and 35800 g/mol, respectively. The PDI (M_w/M_n) was calculated from obtained M_w and M_n values, which is found to be 6.28 and 5.98, respectively. The high-PDI indicated that broad molecular weight distributions are observed in the structure of copolymers. Almost same PDI and average molecular weight were obtained from GPC and intrinsic viscosity methods. This result also suggests that random polymerization reaction occurred via the polycondenzation process, which makes high molecular weight copolymers.

3.4. Thermal Properties of the PCs and Co-PICs. Thermal properties of the PCs and Co-PICs were examined by DSC (exo effect graph) and TG analysis and shown in Figures 7 and 8, respectively. The thermal decomposition behaviour

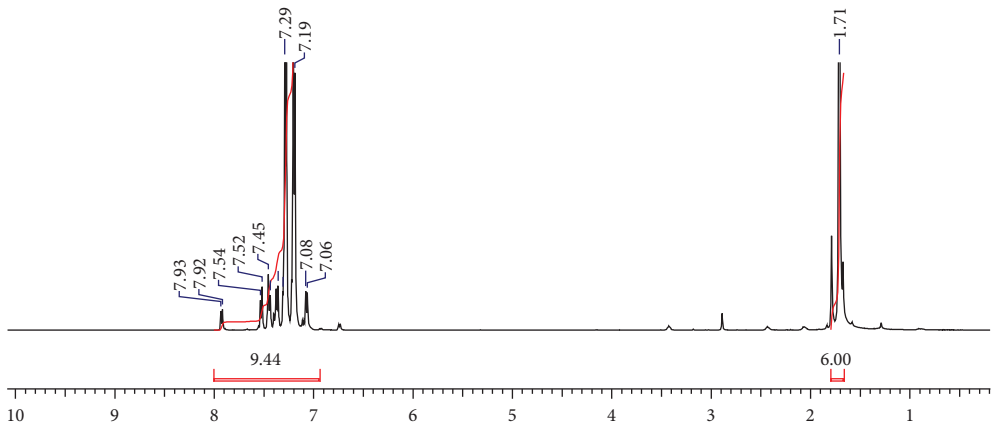

Figure 5: ^{1}H-NMR spectrum of Co-PICs-2.

Table 1: Average molecular weight and poly disperse index of copolymers.

Polymer	Methods	M_n (10^4) (g/mol)	M_w (g/mol)	M_v (g/mol)	PDI
Co-PICs-1	Gel permeation chromatography	6.00	376009	—	6.28
	Intrinsic viscosity	—	—	380189	6.33
Co-PICs-2	Gel permeation chromatography	7.11	358000	—	5.98
	Intrinsic viscosity	—	—	363078	5.10

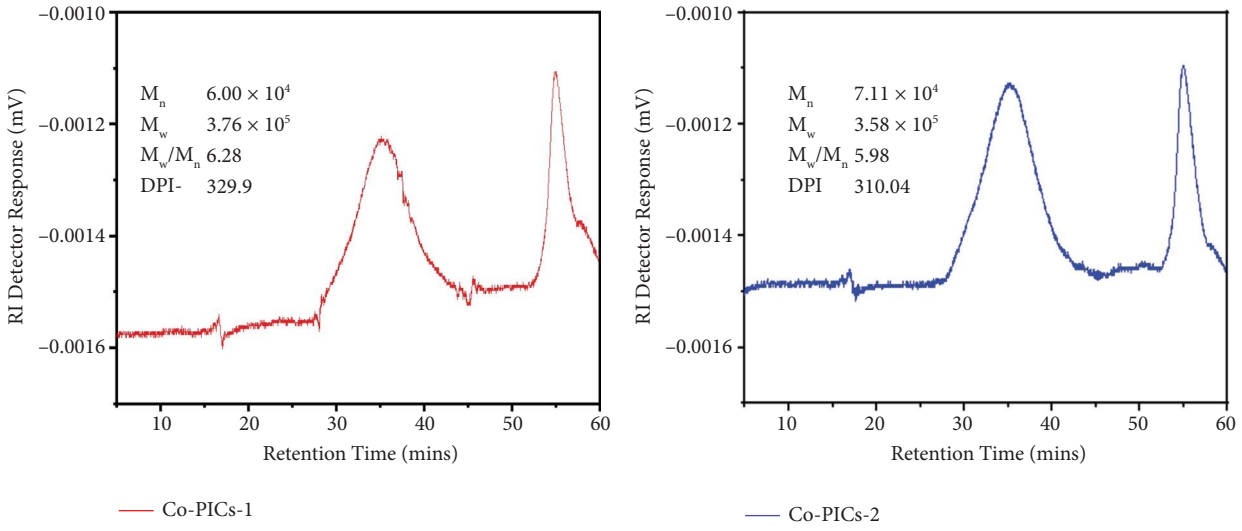

Figure 6: Gel permeation chromatography analysis of (Co-PICs)-1 and (Co-PICs)-2.

and T_g were evaluated under N_2 atmosphere. The glass transition temperatures (T_g) of Co-PICs are increased with the addition of comonomer mole fractions from 143°C for homopolymers (PCs) to 165°C for copolymers. DSC results show that T_g value of copolymers is higher than homopolymers. Slight significant changes occurred in the transparency of homo to copolymer films with 5 to 10 mole % incorporation of comonomers in the polymer structure. So, high heat properties (T_g) are achieved without sacrificing the transparency of PCs. TG analysis shows that PCs (Figure 8) began to decompose at near 400 °C which are less as the thermal decomposing behaviour of Co-PICs (430°C). TG analysis result reveals that the decomposition behaviour of Co-PICs is improved by the incorporation of rigid imide functional moieties in the polymer chain. Based on the DSC and TG analysis, both PCs and Co-PICs are promising materials for FSS substrate due to its more thermal stability.

3.5. Fabrication of Polymer Films. PCs and Co-PICs films were prepared by the solvent casting method and shown in Figure 9. 5% of polymer solution was prepared by dissolving the synthesized polymers into $CHCl_3$. The solution was filtered by using 1 mm PTFE syringe filter and cast on a glass Petri dish. The cast solution was dried at 30°C for 24 hrs to allow slow evaporation of the solvent. Increase the comonomer ratio above 10%, slightly yellow colour was appeared due to the presence of imide moieties in PCs,

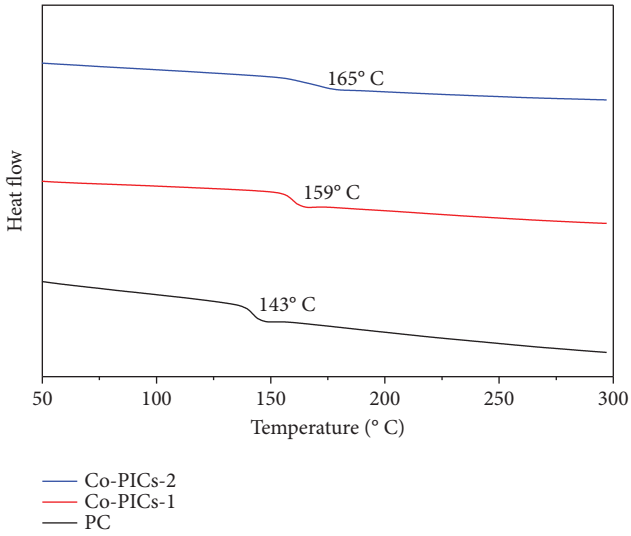

Figure 7: DSC analysis of PC, Co-PICs-1, and Co-PICs-2.

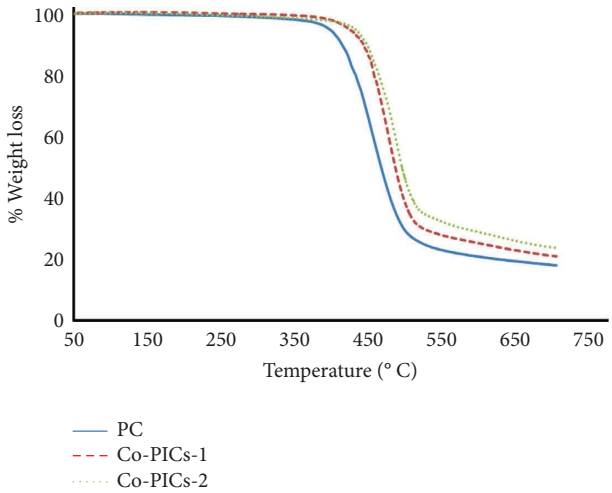

Figure 8: TG analysis of PC, Co-PICs-1, and Co-PICs-2.

which is shown in Figure 9 (Co-PICs-3 comonomer ratio is 15%). The optical transparency of PCs and Co-PICs, Co-PICs-2 was found to be 97.65, 95.75, and 92.64%, respectively (Figure 10). In this study, 2 and 5% optical transparency has decreased for Co-PICs-1, Co-PICs-2, respectively, which is due to the incorporation of comonomers in the polymer structure. The UV results suggest that the comonomer is influenced by optical transparency. Based on the result of PCs and Co-PICs-1, Co-PICs-2 was chosen as a FSS substrate due to its high thermal properties and flexible and optical transparency.

3.6. FSS Design and Analysis. Unit cell design of the FSS geometry was constructed on a polymer substrate of thickness 0.05 mm and is illustrated in Figure 11. The FSS unit cell is of 0.5 mm in thickness with dimensions $P = 15$ mm and $D = 20$ mm. The dielectric constant of the proposed PCs and Co-PICs is found using the dielectric probe kit, and the results are shown in Figure 12. It is evident

Figure 9: Visual representation of thin films of PC (1), Co-PICs-1 (2), and Co-PICs-2 (3).

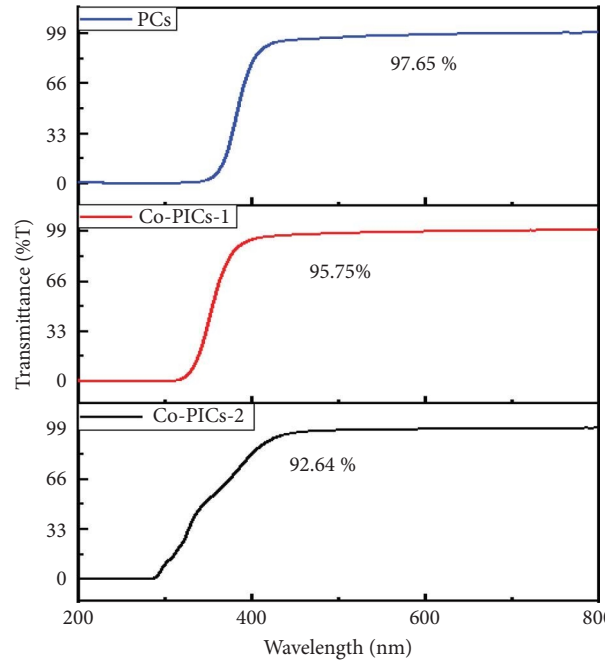

Figure 10: UV-spectral optical transparency of PCs, Co-PICs-1, and Co-PICs-2.

that the increase in mole percentage of comonomer decreases the dielectric constant (ε_r). Hence, for the PCs, Co-PICs-1 and Co- PICs-2 ε_r are found to be 5.8, 5.5, and 4.5 at 8.8 GHz, respectively. The variation in the dielectric value is attributed to the imide linkages which reduces the dielectric constant for increased comonomer ratio. The copolycarbonates (Co-PICs-2) substrate with dielectric constant 4.5 at 8.8 GHz is considered for the analysis. FSS is simulated using the commercially available CST microwave studio software, and its shielding effectiveness (SE) curve is shown in Figure 13. The SE is obtained from the transmission characteristics using the following formula:

$$\text{SE}\,(\text{dB}) = 20 \log \frac{\text{Transmission characteristics without FSS}}{\text{Transmission characteristics with FSS}}. \quad (1)$$

It is apparent from the simulated results that the proposed flexible polymer substrate-based FSS provides band stop response at 8.8 GHz with SE of more than 50 dB for both TE and TM modes of operation. The similar response for TE and TM modes is attributed to the symmetrical geometry of the FSS unit cell, hence providing the advantage of polarization independency.

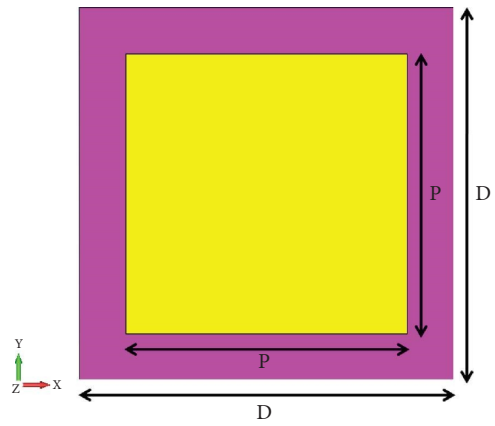

Figure 11: Unit cell geometry of the proposed polymer substrate-based FSS.

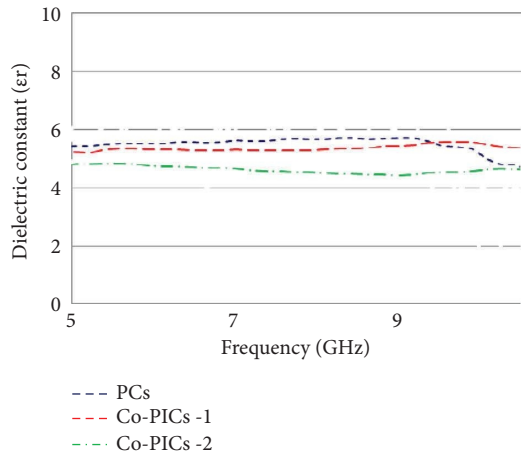

Figure 12: Measured dielectric constants of PCs and Co-PICs substrates.

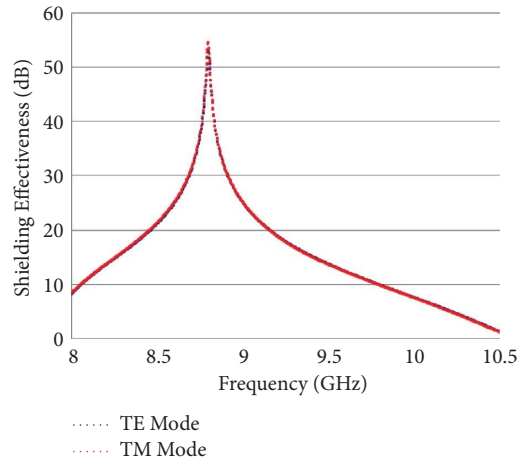

Figure 13: Shielding effectiveness of the proposed polymer (Co-PICs-2)-based FSS.

3.7. FSS Fabrication and Measurement. A prototype of the proposed FSS geometry with polymer substrate has been fabricated and is shown in Figure 14. The FSS unit cells made of copper patches of thickness 0.5 mm are glued to the synthesized Co-PICs-2 substrate. A standard measurement setup consisting of two horn antennas as discussed in [4] is used to measure its performance. Initially, SE of the measurement set up is found without FSS. The measured SE values are normalized with SE obtained after placing the fabricated FSS measured results which are illustrated in Figure 15. It is evident that the measured results are in agreement with the simulated results. Performance

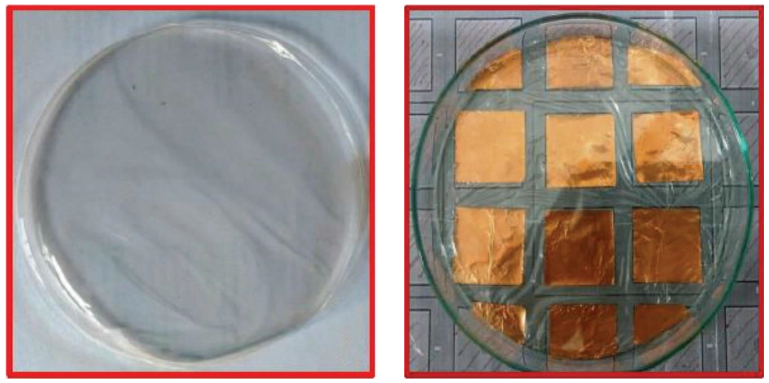

(a) (b)

Figure 14: Co-PICs-2 (a) film and its fabricated FSS (b).

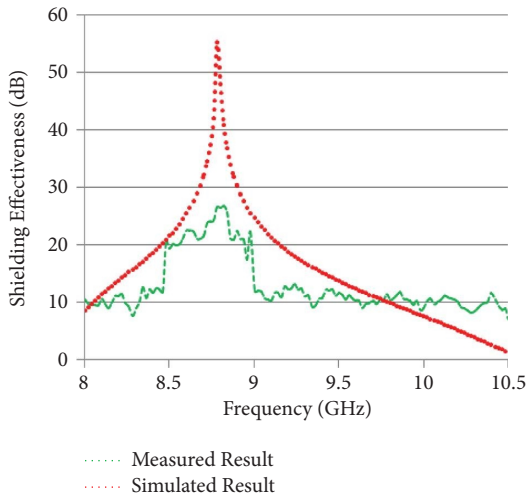

Figure 15: Comparison of the simulated and measured results.

Table 2: Comparison of the proposed polymer-based FSS with FSSs existing in the literature.

Substrate	Dielectric constant (ε_r)	Application	Ref.
Polyethylene terephthalate (PET)	2.7	Shielding X band 10 GHz	[39]
Paper	3.4	Shielding GSM bands 930 and 1720 MHz	[40]
Polyethylene terephthalate (PET)	2.2	Shield 1.8 GHz	[41]
Co-PICs-2	4.5	Shield 8.8 GHz	Present work

comparison of the proposed polymer-based FSS with the existing FSSs is provided in Table 2. It is observed that the proposed polymer-based FSS provides shielding up to 20 dB in the desired spectrum. The fabricated flexible polymer-based FSS is found to be the potential candidate for shielding conformal surfaces providing good transparency against its conventionally used FR-4 substrate.

4. Conclusions

Flexible PCs and Co-PICs were successfully synthesized by the melt polycondenzation process. The imide, ether, and methyl functional moieties were incorporated in the structure of copolycarbonates, which was confirmed by FT-IR and NMR analysis. DSC and TG analyses were used to examine the thermal properties of PCs and Co-PICs. The results showed that the T_g and T_d of Co-PICs were improved from 143 to 165°C and from 400 to 430°C, respectively, compared to PCs. This indicates that Co-PICs are more stable even at high temperatures without compromising the standard properties of PCs. The polymer thin film was prepared by the solvent casting method using $CHCl_3$. Based on the dielectric constant result, Co-PICs-2 is chosen as a substrate in FSS design. A prototype of the FSS is fabricated, and the measured results are found to be in good agreement with simulated results. The good thermal stability, flexibility, transparency, and simulation measurement of Co-PICs indicated that the Co-PICs could offer excellent

substrate and stable polymeric materials to be used for the design of flexible FSS, which finds wide applications in the field of electromagnetic shielding.

Data Availability

Data are available on request.

Conflicts of Interest

The authors declare that they have no conflicts of interest.

Supplementary Materials

Figure S1. ^{1}H-NMR spectrum of compound BPA. Figure S2. ^{1}H-NMR spectrum of compound DPC. Figure S3. ^{1}H-NMR spectrum of polycarbonates. Figure S4. ^{13}C-NMR spectrum of polycarbonates. (*Supplementary Materials*)

References

[1] G. Allen and J. C. Bevington, *Comprehensive Polymer Science: The Synthesis, Characterization, Reactions & Applications of Polymers*, Pergamon Press, Oxford, England, 1989.

[2] J. Cayuela, F. Da Cruz-Boisson, A. Michel, P. Cassagnau, and V. Bounor-Legaré, "Synthesis of bisphenol-A polycarbonate-poly (ε-caprolactone) copolymers by reactive extrusion through in situ ε-caprolactone polymerization," *Polymer*, vol. 104, pp. 156–169, 2016.

[3] L. J. Broutman and S. M. Krishnakumar, "Impact strength of polymers: 1. The effect of thermal treatment and residual stress," *Polymer Engineering & Science*, vol. 16, no. 2, pp. 74–81, 1976.

[4] S. Bigot, N. Kebir, L. Plasseraud, and F. Burel, "Organo-catalytic synthesis of new telechelic polycarbonates and study of their chemical reactivity," *Polymer*, vol. 66, pp. 127–134, 2015.

[5] J. Jakobsen, M. Jensen, and J. H. Andreasen, "Thermo-mechanical characterisation of in-plane properties for CSM E-glass epoxy polymer composite materials – Part 1: thermal and chemical strain," *Polymer Testing*, vol. 32, no. 8, pp. 1350–1357, 2013.

[6] S. Ramprabhu, M. Lingeshwaran, K. Malathi, S. Esther Florence, and M. Gulam Nabi Alsath, "Letters," *IEEE Transactions on Electromagnetic Compatibility*, vol. 58, no. 2, pp. 611–614, 2016.

[7] T. Kobayashi and L. J. Broutman, "Cold rolling of polymers 3. Properties of rolled crystallized polycarbonates," *Polymer Engineering & Science*, vol. 14, no. 4, pp. 260–263, 1974.

[8] B. Yin, Y. Zhao, W. Yang, M. M. Pan, and M. B. Yang, "Polycarbonate/liquid crystalline polymer blend: crystallization of polycarbonate," *Polymer*, vol. 47, no. 25, pp. 8237–8240, 2006.

[9] L. J. Broutman and S. M. Krishnakumar, "Cold rolling of polymers 2. Toughness enhancement in amorphous polycarbonates," *Polymer Engineering & Science*, vol. 14, no. 4, pp. 249–259, 1974.

[10] V. Sivakumar and B. Rajamouli, "Molecular designing of luminescent europium-metal complexes for OLEDs: an overview," *Phosphors*, Jenny Stanford Publishing, New York, NY, USApp. 325–404, 2018.

[11] T. Wang, M. Yan, X. Sun, and D. Quan, "The mechanical and biological properties of polycarbonate-modified F127 hydrogels after incorporating active pendent double-bonds," *Polymer*, vol. 57, pp. 21–28, 2015.

[12] E. Y. Choi, J. Y. Kim, and C. K. Kim, "Fabrication, and properties of polycarbonate composites with polycarbonate grafted multi-walled carbon nanotubes by reactive extrusion," *Polymer*, vol. 60, pp. 18–25, 2015.

[13] M. Colonna and M. Fiorini, "Solid state polymerization of bisphenol A polycarbonate: effect of the crystallization method and polymerization conditions," *Polymer Engineering & Science*, vol. 55, no. 5, pp. 1024–1029, 2015.

[14] J. T. Ryan, "Impact and yield properties of polycarbonate as a function of strain rate, molecular weight, thermal history, and temperature," *Polymer Engineering & Science*, vol. 18, no. 4, pp. 264–267, 1978.

[15] X. Li and A. F. Yee, "Design of mechanically robust high-T g polymers: synthesis and dynamic mechanical relaxation behavior of glassy poly (ester carbonate) s with cyclohexylene rings in the backbone," *Macromolecules*, vol. 36, no. 25, pp. 9411–9420, 2003.

[16] M. Ueda, "A study on the characteristics of antiplasticized polycarbonates and their optical disk substrates," *Polymer Engineering & Science*, vol. 44, no. 10, pp. 1877–1884, 2004.

[17] E. J. Dziwiński, J. Iłowska, and J. Gniady, "Py-GC/MS analyses of poly (ethylene terephthalate) film without and with the presence of tetramethylammonium acetate reagent. Comparative study," *Polymer Testing*, vol. 65, pp. 111–115, 2018.

[18] G. Deng, H. Huang, P. Si et al., "Synthesis and electro-optic activities of novel polycarbonates bearing tricyanopyrroline-based nonlinear optical chromophores with excellent thermal stability of dipole alignment," *Polymer*, vol. 54, no. 23, pp. 6349–6356, 2013.

[19] F. C. Chiu, Y. C. Chuang, S. J. Liao, and Y. H. Chang, "Comparison of PVDF/PVAc/GNP and PVDF/PVAc/CNT ternary nanocomposites: enhanced thermal/electrical properties and rigidity," *Polymer Testing*, vol. 65, pp. 197–205, 2018.

[20] Y. Liang, X. Zhou, Y. Liao, J. Wu, X. Xie, and H. Zhou, "Reactive polycarbonate/diallyl phthalate blends with high optical transparency, good flowability and high mechanical properties," *Polymer*, vol. 91, pp. 89–97, 2016.

[21] T. Chen, L. Pan, M. Lin et al., "Dielectric, mechanical and electro-stimulus response properties studies of polyurethane dielectric elastomer modified by carbon nanotube-graphene nanosheet hybrid fillers," *Polymer Testing*, vol. 47, pp. 4–11, 2015.

[22] J. Huang, C. He, X. Li, G. Pan, and H. Tong, "Theoretical studies on thermal degradation reaction mechanism of model compound of bisphenol A polycarbonate," *Waste Management*, vol. 71, pp. 181–191, 2018.

[23] E. Moretti, M. Zinzi, and E. Belloni, "Polycarbonate panels for buildings: experimental investigation of thermal and optical performance," *Energy and Buildings*, vol. 70, pp. 23–35, 2014.

[24] F. C. Chiu, "Poly (vinylidene fluoride)/polycarbonate blend-based nanocomposites with enhanced rigidity—selective localization of carbon nanofillers and organoclay," *Polymer Testing*, vol. 62, pp. 115–123, 2017.

[25] Z. Xiaozhou, L. Yang, L. Xin, L. Xin, J. Xigao, and W. Jinyan, "Improving the thermal properties of polycarbonate via the copolymerization of a small amount of bisphenol fluorene with bisphenol A, 2022," *International Journal of Polymer Science*.

[26] S. Suin, S. Maiti, N. K. Shrivastava, and B. B. Khatua, "Mechanically improved and optically transparent

polycarbonate/clay nanocomposites using phosphonium modified organoclay," *Materials & Design*, vol. 54, pp. 553–563, 2014.

[27] E. Moretti, M. Zinzi, E. Carnielo, and F. Merli, "Advanced polycarbonate transparent systems with aerogel: preliminary characterization of optical and thermal properties," *Energy Procedia*, vol. 113, pp. 9–16, 2017.

[28] Z. Cai, H. Yu, Y. Zhang et al., "Synthesis and characterization of novel fluorinated polycarbonate negative-type photoresist for optical waveguide," *Polymer*, vol. 61, pp. 140–146, 2015.

[29] M. M. Sayyed and N. N. Maldar, "Novel poly (arylene-ether-ether-ketone) s containing preformed imide unit and pendant long chain alkyl group," *Materials Science and Engineering: B*, vol. 168, no. 1-3, pp. 164–170, 2010.

[30] J. Cao, W. Su, Z. Wu, J. Liu, T. Kitayama, and K. Hatada, "Crystallization behaviour of poly (ether ether ketone)/poly (ether sulfone) block copolymer," *Polymer*, vol. 37, no. 20, pp. 4579–4584, 1996.

[31] S. D. Hudson, D. D. Davis, and A. J. Lovinger, "Semi-crystalline morphology of poly (aryl ether ether ketone)/poly (ether imide) blends," *Macromolecules*, vol. 25, no. 6, pp. 1759–1765, 1992.

[32] R. Sivasamy and M. Kanagasabai, "Novel reconfigurable 3-D frequency selective surface," *IEEE Transactions on Components, Packaging, and Manufacturing Technology*, vol. 7, no. 10, pp. 1678–1682, 2017.

[33] M. U. Ali Khan, R. Raad, F. Tubbal, P. I. Theoharis, S. Liu, and J. Foroughi, "Bending analysis of polymer-based flexible antennas for wearable, general IoT applications: a review," *Polymers*, vol. 13, no. 3, p. 357, 2021.

[34] R. Natarajan, M. Kanagasabai, S. Baisakhiya, R. Sivasamy, S. Palaniswamy, and J. K. Pakkathillam, "A compact frequency selective surface with stable response for WLAN applications," *IEEE Antennas and Wireless Propagation Letters*, vol. 12, pp. 718–720, 2013.

[35] R. Sivasamy, B. Moorthy, M. Kanagasabai, V. R. Samsingh, and M. G. N. Alsath, "A wideband frequency tunable FSS for electromagnetic shielding applications," *IEEE Transactions on Electromagnetic Compatibility*, vol. 60, no. 1, pp. 280–283, 2018.

[36] S. Maudgal, J. R. Pratt, N. T. Wakelyn, and T. L. St Clair, "Synthesis and properties of copoly (carbonate imides)," *Polymer Engineering & Science*, vol. 25, no. 4, pp. 245–249, 1985.

[37] M. Sato, T. Hirata, and K. I. Mukaida, "Thermotropic liquid-crystalline aromatic-aliphatic polyimides, 1. Novel poly (imide-carbonate) s containing pyromellitimide ring," *Makromolekulare Chemie*, vol. 193, no. 7, pp. 1729–1737, 1992.

[38] K. Matyjaszewski, "The synthesis of functional star copolymers as an illustration of the importance of controlling polymer structures in the design of new materials," *Polymer International*, vol. 52, no. 10, pp. 1559–1565, 2003.

[39] W. Y. Yong, T. Hartman, and A. A. Glazunov, "Flexible low profile frequency selective surface for X-band shielding applications," in *Proceedings of the Joint International Symposium on Electromagnetic Compatibility, Sapporo and Asia-Pacific International Symposium on Electromagnetic Compatibility (EMC Sapporo/APEMC)*, pp. 435–438, Sapporo, Japan, June 2019.

[40] R. Sivasamy, L. Murugasamy, M. Kanagasabai, E. F. Sundarsingh, and M. Gulam Nabi Alsath, "A low-profile paper substrate-based dual-band FSS for GSM shielding," *IEEE Transactions on Electromagnetic Compatibility*, vol. 58, no. 2, pp. 611–614, 2016.

[41] L. B. Wang, K. Y. See, J. W. Zhang, B. Salam, and A. C. W. Lu, "Ultrathin and flexible screen-printed metasurfaces for EMI shielding applications," *IEEE Transactions on Electromagnetic Compatibility*, vol. 53, no. 3, pp. 700–705, 2011.